Journal of ELECTRONIC MATERIALS, Vol. 45, No. 8, 2016
DOI: 10.1007/s11664-016-4543-0

Analysis of an Increase in the Efficiency of a Spark Ignition Engine Through the Application of an Automotive Thermoelectric Generator

JERZY MERKISZ,[1] PAWEL FUC,[1] PIOTR LIJEWSKI,[1] ANDRZEJ ZIOLKOWSKI,[1,2] MARTA GALANT,[1] and MACIEJ SIEDLECKI[1]

1.—Faculty of Machines and Transport, Institute of Combustion Engines and Transport, Poznan University of Technology, Piotrowo st. 3, 60-965 Poznan, Poland. 2.—e-mail: andrzej.j.ziolkowski@put.poznan.pl

We have analyzed the increase of the overall efficiency of a spark ignition engine through energy recovery following the application of an automotive thermoelectric generator (ATEG) of our own design. The design of the generator was developed following emission investigations during vehicle driving under city traffic conditions. The measurement points were defined by actual operation conditions (engine speed and load), subsequently reproduced on an engine dynamometer. Both the vehicle used in the on-road tests and the engine dynamometer were fit with the same, downsized spark ignition engine (with high effective power-to-displacement ratio). The thermodynamic parameters of the exhaust gases (temperature and exhaust gas mass flow) were measured on the engine testbed, along with the fuel consumption and electric current generated by the thermoelectric modules. On this basis, the power of the ATEG and its impact on overall engine efficiency were determined.

Key words: Waste heat recovery, engine efficiency, ATEG, RDE

INTRODUCTION

According to the sustainable development policy implemented within the framework of the Europe 2020 strategy, it is necessary to reduce consumption of conventional energy sources (oil, gas, and coal) to build a competitive, low-carbon economy.[1,2] This policy is implemented through a number of legal norms that imply limiting emissions of greenhouse gases (GHGs), especially CO_2. In 2007, the European Commission (EC) proposed a 30% reduction of greenhouse-gas emissions in developed countries by the year 2020, and suggested that the European Union itself should make a firm independent commitment to achieve at least a 20% reduction in greenhouse-gas emissions.[2] For the automotive industry, road emissions standards were introduced for either CO_2 emission or fuel consumption (Table I).

According to Aren et al.,[1] CO_2 emissions from the road transport sector constitute 16.4% of global emissions. Powering vehicles is currently responsible for 38% of annual global demand for oil.[1]

To meet such CO_2 emissions limits, road-vehicle manufacturers will have to implement new, innovative solutions. Currently, the basic directions of development of spark ignition (SI) engines are downsizing, use of gasoline direct injection systems, as well as variable valve timing and valve lift. A variable geometric compression ratio during engine operation is also used. There are two types of downsizing: static and dynamic.[3] Static downsizing typically refers to reduction of the geometric dimensions of the engine—often by reducing the number of cylinders or displacement volume. Another possibility is to deactivate cylinders during the combustion engine work cycle—known as dynamic downsizing.

(Received September 9, 2015; accepted April 12, 2016; published online May 19, 2016)

Table I. CO_2 emission and fuel consumption norms around the world[1]

Country or region	Target year	Standard type	Unadjusted fleet target	Test cycle	Penalties
EU	2015	CO_2	130 gCO_2/km	NEDC (WLTP from 2017)	Economic fines
	2021		90 gCO_2/km	WLTP	
Japan	2015	Fuel economy	16.8 km/dm^3	JC08	Economic fines
	2020		20.3 km/dm^3		Public proclamation
Canada	2016	CO_2 + other GHGs	217 gCO_2/mi	US combined	Economic fines
	2025 (proposed)		N/A		Sales restriction
India	From 2016	CO_2	(130 g/km)	NEDC for low-powered vehicle	Not available
	2021		113 g/km		
China	2015	Fuel consumption	6.9 dm^3/100 km	NEDC	Economic fines
	2020 (proposed)		5 dm^3/100 km		Public proclamation
USA	2016	Fuel economy/CO_2 + other GHGs	36.2 mpg or 225 g/CO_2 km	US combined	Economic fines
	2025		56.2 mpg or 143 gCO_2/km		Sales restriction
South Korea	2015	Fuel economy/CO_2 + other GHGs	17 km/dm^3 or 140 gCO_2/km	US combined	Public proclamation
Mexico	2016	Fuel economy/CO_2 + other GHGs	39.3 mpg or 140 gCO_2/km	US combined	Economic fines

The aforementioned methods aim to increase the overall efficiency of the engine, thereby reducing its fuel consumption while maintaining the generated power output.[4] Most of the chemical energy contained in the fuel is drained through the cooling system, as well as in the form of heat and pressure in exhaust gases. There is great potential for heat energy recovery from exhaust gases, as its share in the energy balance for SI engines can be as high as 45%. For CI engines, it is assumed that the share of thermal energy loss in the exhaust gases is a maximum of 35%. For this reason, systems that work in the Clausius–Rankine cycle as well as thermoelectric generators for automotive applications (ATEGs) have been developed and implemented.[5–10]

CHOOSING A COMBUSTION ENGINE FOR RESEARCH

For analysis of increased spark ignition (SI) engine efficiency through heat recovery from exhaust gases using an ATEG, Volkswagen's modern TSI 1.2-dm^3 engine was selected (Fig. 1). This engine is a consequence of the strategy adopted by the company, which relies on implementation of engine downsizing. One of the first solutions of this type was the TSI 1.4-dm^3 engine. The selected combustion engine was primarily developed to meet CO_2 emissions requirements. According to the manufacturer,* the Audi A3 vehicle, equipped with two versions of the model TFSI 1.2-l engine with power of 63 kW and 77 kW, reaches CO_2 emissions of 118 g/km and 127 g/km, respectively, in the NEDC test. These values are significantly lower than the established limit, which in 2015 equals 130 g/km.

Fig. 1. 1.2-dm^3 TSI combustion engine chosen for this research.

The engine block is made of aluminum with innovative cast-iron cylinder liners. It uses two valves per cylinder. The inlet valve jacks have a special shape, which is responsible for producing a swirl type of turbulence that facilitates formation of a homogeneous air–fuel mixture. The engine crankshaft is made of steel with reduced diameter of the main journal and crank bearings with light connecting rods, which is meant to reduce friction losses. The engine has a gasoline direct injection

*Information from the vehicle producer.

system with six-hole injectors that generate injection pressure of 45 bar to 125 bar. To achieve high volumetric power, the engine is equipped with a turbocharger with an exhaust wastegate valve.

To determine the actual driving profile as a function $V = f(t)$, tests under actual operating conditions were performed using advanced research tools, including a portable emissions measurement system (PEMS). The tests were performed on a test route with total length of 12.6 km. When selecting the test route, the authors aimed to reproduce typical urban (involving frequent vehicle stops) and suburban conditions. The selected test route met the said requirements. The "urban" part included highly congested streets and involved a variety of intersections. The "suburban" part was a portion of the road number 92—one of the main eastern entrance roads to the Poznan agglomeration. Such varied road conditions allow analyses to be conducted under a wide range of speeds and varied accelerations. This influences the effective engine parameters, which translate directly into the amount of thermal energy in the exhaust gases.

DETERMINING THE POWER BAND OF THE ENGINE BASED ON MEASUREMENTS MADE WITH THE RDE METHODOLOGY

To determine the engine power band for test bench investigation of the heat recovery from the exhaust gases, tests were carried out under real operating conditions in accordance with the real driving emissions (RDE) methodology. This study selected a vehicle equipped with a 1.2-dm^3 TSI engine, which was also located on an engine dyno station. Measurements were made using the latest PEMS instrument—the SEMTECH ECOSTAR. This is another device from the SEMTECH® series—a successor to the SEMTECH DS analyzer. The main difference between these devices is that the SEMTECH ECOSTAR is made up of separate modules (Fig. 2):[11]

1. Fuel economy meter (FEM) module for measuring the concentration of CO_2, CO, and total hydrocarbons (THC) using a nondispersive infrared (NDIR) analyzer,
2. NO_x module for measurement of NO_x (NO and NO_2) concentrations using a nondispersive ultraviolet (NDUV) analyzer,
3. Flame ionization detector (FID) module to measure THC,
4. Power distribution module (PDM) to supply power to each component.

When all the modules (of the gas measurement section) are used, they must be connected together by a controller area network (CAN; green lines in Fig. 3). The FEM module is connected via a special cable to a flow meter for measuring thermodynamic parameters of exhaust gases (mass flow, temperature, and pressure). This line is supplied a sample of exhaust gases that passed through the NDIR analyzer (measuring CO_2, CO, and THC), directed to the NO_x module with three connectors, wherein measurements of NO and NO_2 take place. Apart from the exhaust gas sample, a special conduit transmits the signal from the vehicle global positioning system (GPS) and a weather sensor used to measure atmospheric conditions (temperature, pressure, and humidity), which are connected to the flow meter. A computer for system control and a signal converter from the vehicle's diagnostic system are connected using an AUX2 connector to the PDM, FEM, and NO_x modules. Each module is equipped with one AUX1 and one AUX2 connection point. The signal from the power supply module for the heated wire is sent to the FID module. The SEMTECH ECOSTAR device can be powered by a PDM module, to which voltage is supplied from the grid or the car battery. It is also possible to directly

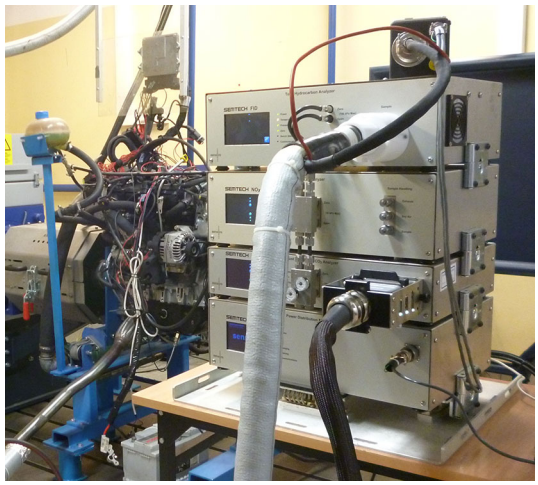

Fig. 2. SEMTECH ECOSTAR instrument, used to measure emissions in accordance with the RDE methodology.

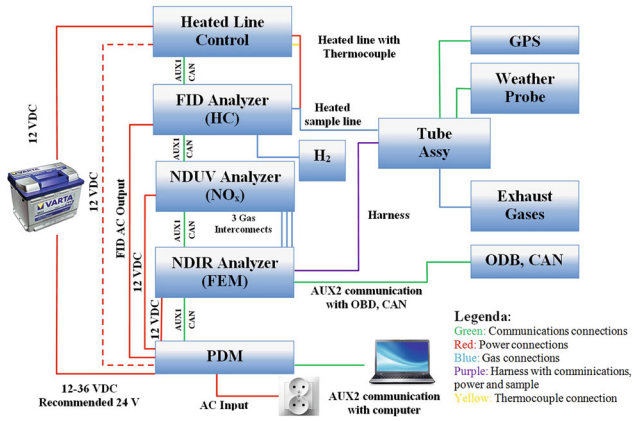

Fig. 3. Diagram of SEMTECH ECOSTAR system used for testing—section responsible for measurement of gaseous compounds.

connect the modules to the mains. Due to the modular design of the instrument, it can perform measurements of all gaseous compounds simultaneously, or separately using single modules.

For the purposes of this study, only measurements of CO_2 and CO (FEM module), thermodynamic parameters of exhaust gases (temperature, pressure, and mass flow rate), as well as weather conditions and vehicle speed and position were taken. These measurements were performed under real operating conditions on a designated route with length of 12 km. A detailed description of the test route is given in Refs. 8 and 12. Measurements were carried out on a weekday afternoon.

On the basis of the measurements taken in accordance with the RDE methodology, the characteristics of the share of working time intervals in relation to crankshaft speed and engine load for the tested vehicle were determined, as presented in a three-dimensional (3D) graph in Fig. 4. The power band of engine operation was defined as the average time in the range of 400 rpm and 20 Nm. For more than half of the total test time, the engine was in the range of 1400 rpm to 3000 rpm with load not exceeding 100 Nm. Single points of work, whose share accounted for only 3%, were recorded above this range. The share of idling time amounted to 31%.

The registered operating points of the combustion engine are presented with the full power characteristic as a two-dimensional (2D) graph in Fig. 5, from which it can be determined that the engine was mainly operating in the crankshaft rotational speed range of 1500 rpm to 3500 rpm, where the torque is maximum. The combustion engine did not reach the value of 177 Nm. The maximum torque obtained in the road test was 144 Nm. No operating points were registered in the range of maximum engine crankshaft speed. This distribution of engine operating points stems directly from the route used in the test. The route has an urban section, where the vehicle speed limit is 50 km/h, and a suburban section, where the limit is 70 km/h. There are also parts of the route which have a 30 km/h or 40 km/h speed limit. As a result of this, the vehicle cannot obtain a high average speed during the test cycle, which results in the engine operating at low and medium loads. During the research, the vehicle reached a maximum speed of 77 km/h and its average speed was 33.2 km/h.

To best mimic the registered working conditions of the test vehicle's drive unit when testing on the engine dyno bench, it was decided that the research would be carried out at three different load characteristics with a constant speed of the engine crankshaft with load changed in 20-Nm intervals (Fig. 5, marked with pink dots): 1800 rpm (six operating points), 2200 rpm (five operating points), and 2800 rpm (four operating points). The study also included the engine idling state (800 rpm). This gives a total of 16 operating points for the engine, at which tests were carried out under laboratory conditions.

RESEARCH METHODOLOGY USED FOR ENGINE DYNO TEST BENCH

Measurements of heat recovery from the exhaust gases were carried out on a static engine dyno test bench from Automex company, on which the 1.2-dm^3 TSI engine was mounted, generating a maximum power output of 77 kW at 5000 rpm (Table II). The volumetric power indicator of this drive unit is 64.2 kW/dm^3. The engine meets the Euro 5 emission standards and is equipped with a three-way catalytic (TWC) converter.

The study used the prototype ATEG developed by the authors as part of the Applied Research Programme funded by the National Centre for Research and Development (Fig. 6; Table III). This ATEG is modular and consists of three main elements: a heat exchanger, commercial thermoelectric modules, and cooling elements. The main

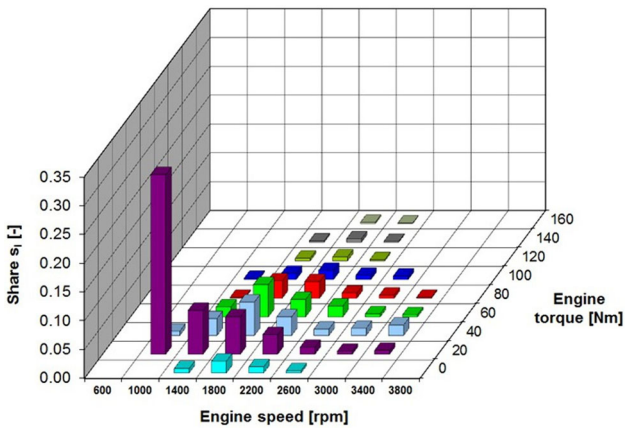

Fig. 4. Time share characteristics in the range of engine crankshaft speeds and loads in a test carried out in accordance with RDE methods.

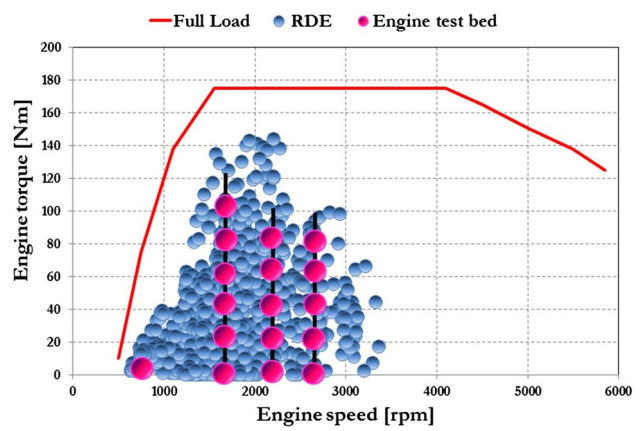

Fig. 5. Operating points for the engine of the test vehicle achieved in a test carried out in accordance with RDE methods with its full power characteristic.

Table II. Parameters of the tested 1.2-dm^3 TSI engine

Parameter	Value
Type of engine	Spark ignition
Displacement	1.2 dm^3
Number of cylinders	4
Stroke	75.6 mm
Bore	71 mm
Number of valves per cylinder	2
Power output	77 kW at 5000 rpm
Torque	175 Nm at 1550 rpm to 4100 rpm
Emissions standard	Euro 5
Exhaust gas posttreatment	TWC with lambda control

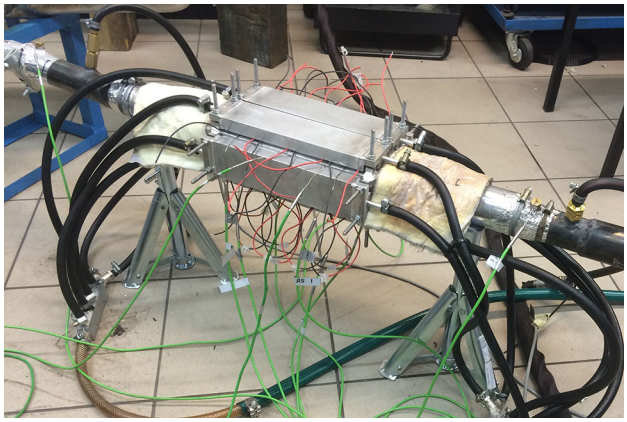

Fig. 6. ATEG installed in the engine testbed.

part of the heat exchanger, onto which the thermoelectric modules are arranged, has a rectangular shape.

Its width is almost twice its height. To ensure a uniform temperature distribution along the heat exchanger, ribbing with increasing cross-section was implemented inside it. It was assumed that four modules were arranged longitudinally on each side of the heat exchanger. There are two rows of modules on the top and bottom sides of the heat exchanger, and one row on each side, for a total of 24 modules. There is one dedicated cooling panel for each row of modules, attached to the heat exchanger by means of a screw connection. Each radiator is screwed to a heat exchanger using four screws placed at its corners. To ensure uniform pressure of the modules on the wall of the exchanger, an additional locking system was also used in the middle of the radiators. The screws were tightened to maximum torque of 20 Nm. This allows use of thermoelectric modules of different thickness. A special silicated thermal grease was applied between the modules and the walls of the heat exchanger to facilitate heat transfer from the walls

Table III. ATEG characteristics

Parameter	Value
Length	671 mm
Width	200 mm
Height	135 mm
Inlet diameter	60 mm
Material	Aluminum alloy with thickness of 2 mm
Number of modules	24
Module arrangement	Top and bottom walls—two rows with four modules each; side walls—one row with four modules
Type of modules used	TMG-241-1.4-1.2 by Ferrotec NORD
Number of cooling panels	6
Generated nominal power	225.6 W
Generated nominal voltage without load	300 V
Generated nominal voltage with load	151.2 V

of the heat exchanger to the hot side of the module and help reduce possible heat leaks arising from the surface roughness of the heat exchanger and other material imperfections and faults.

The study used 24 commercial Ferrotec SCTB NORD thermoelectric modules codenamed TMG-241-1.4-1.2,[13] connected in series. These modules are Bi_2Te_3 based, and each can generate 9.4 W of power. The maximum temperature of the hot side of the module may not exceed 200°C when using thermally conductive paste. Without conductive paste, the temperature should not exceed 175°C. The module generates a maximum voltage of 12.5 V with no load, and 6.3 V with load. The modules were chosen based on previous research experience of the authors with heat recovery from exhaust gases using ATEG. Reference[8] presents the results of a TEG with a different design, using an earlier version of the TMG-241-1.4-1.2 modules, whose maximum power was 7 W. These were selected on the basis of measurements showing that they achieved satisfactory operating parameters while maintaining resistance to the effects of high temperatures. The TMG-241-1.4-1.2 modules are characterized by high durability due to the nature of the joining techniques, junction materials, and diffusion barriers. For this reason, in the prototype ATEG which is the subject of this study, the authors used a newer version of the TMG-241-1.4-1.2 modules from SCTB NORD A Ferrotec Group Company. During the tests of heat recovery from exhaust gases performed on the static engine test bench, the following parameters were measured:

(a) Instantaneous fuel consumption G (g/s), using a mass fuel gauge from Automex company,

(b) Crankshaft rotational speed s (rpm) and engine torque T (Nm), using the stationary engine dyno test bench made by Automex company, equipped with an eddy-current brake and inductive engine speed sensor,
(c) Exhaust mass flow rate EFM (kg/h), using the SEMTECH ECOSTAR,
(d) Exhaust gas temperature at four measurement points t_1, t_2, t_3, and t_4 (°C), using thermocouples,
(e) Temperature of the hot side of the thermoelectric modules t_{11}, t_{12}, t_{21}, t_{22}, t_{31}, t_{32}, t_{41}, t_{42}, t_{51}, t_{52}, t_{61}, and t_{62} (°C) (first and last module in each row), using thermocouples,
(f) Mass flow m_{cool} (dm^3/h) and temperature t_{cool} (°C) of the coolant,
(g) Voltage U (V) and current I (A) generated by the modules, using a custom-made measurement system of the authors' design.

To register the temperatures and pressures, two IOTECH Personal Daq/3000 signal converters were used. The measurement module was equipped with a universal serial bus (USB) interface and high-speed analog-to-digital (A/D) converter (1 MHz/16 bit). The transmitter has 16 single-ended-type analog inputs (8 differential inputs), 4 analog outputs, and 24 digital input/output lines, and it is possible to program the device in seven ranges from ±100 mV to ±10 V. Information from the sensor is transmitted to a computer, which records the data at a given frequency.

The custom measurement system to measure the voltage and current generated by the modules consists of: the main module (which includes, among others, a USB-600 measuring card manufactured by National Instruments having eight analog inputs and four digital inputs), two converters for voltage and current measurements fitted on a printed circuit board (PCB), a slide resistor for setting the load of the system, as well as control software. The main module is supplied with a voltage of 220 V. The software allows for monitoring of the generated voltage and current in real time (in numerical and graphical form) as well as data recording at a frequency of 1 Hz. It uses algorithms to calculate the generated power in watts and the energy expressed in kWh. A measuring device records the total value of voltage and current of all modules, but also has the ability to measure these values for individual modules.

ANALYSIS OF RESULTS

The overall efficiency of an internal combustion engine is a measure of its use of the energy contained in the fuel. It provides insight into the conversion efficiency of chemical energy contained in the fuel into mechanical energy output by the motor to the power receiver. This efficiency is also described as the inverse of the specific fuel consumption and can be expressed by the formula

$$\eta_0 = \frac{P_e}{G \cdot \mathrm{GCV}} = \frac{1}{\mathrm{BSFC} \cdot \mathrm{GCV}}, \quad (1)$$

where η_0 is the overall efficiency (–), P_e is the engine power output (kW), G is the instantaneous fuel consumption (g/s), BSFC is the specific fuel consumption (g/kWh), and GCV is the gross calorific value (J/g).

To determine the total efficiency of an internal combustion engine using an ATEG, the power generated by the generator P_{eATEG} needs to be included in Eq. 1, as follows:

$$\eta_{E+ATEG} = \frac{(P_e + P_{ATEG})}{G \cdot \mathrm{GCV}} = \frac{[P_e + (U \cdot I)_{ATEG}]}{G \cdot \mathrm{GCV}}. \quad (2)$$

Such addition of the power generated by the ATEG P_{eATEG} to the power output of the engine P_e is justified because the generator produces electrical power from the thermal energy of the exhaust gases after fuel combustion, which in an internal combustion engine is treated as waste as the heat created by burning the air–fuel mixture is not used. This increases the overall efficiency of the engine, because a greater amount of energy is obtained from the combustion produced by the same amount of fuel. In this way, the heat loss in the exhaust gases is also limited.

The determination of the overall engine efficiency on the engine dyno bench used the measured parameters of crankshaft speed and engine load (used to calculate the engine power output) and the fuel consumption per second G_s. This consumption can also be calculated from the emissions per second of CO_2, CO, and THC in accordance with the carbon balance method as modified by the authors.[14] As part of the tests carried out, the relationship between the fuel consumption (as measured by Automex instrumentation) and the consumption calculated on the basis of the parameters measured by the PEMS equipment was determined; more than 30 trials were performed for each operating point of the engine, which statistically can be treated as a large test sample. Figure 7 shows the relationship between the average values of instanteneous fuel consumption for the three engine speeds.

The datasets were linearly interpolated, obtaining a coefficient of determination R^2 close to 1. This reveals very good agreement between the results obtained using the two methods. Thus, the carbon balance method to calculate the fuel consumption per second is shown to be reliable and can be used for results obtained both on the engine dyno bench and under real conditions (RDE methodology).

The specific fuel consumption in the studies conducted was in the range of 238.5 g/kWh to 384.4 g/kWh (Table IV). The lowest value indicates the highest overall efficiency of the engine, which

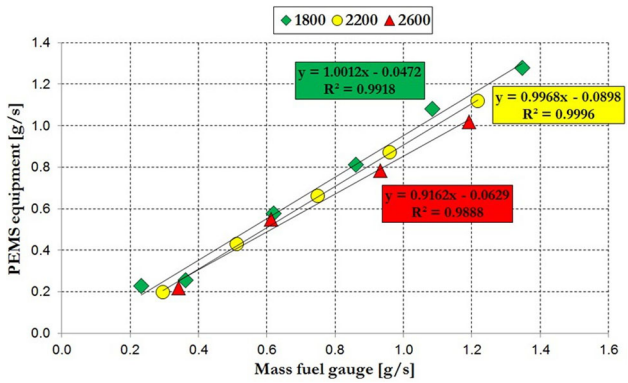

Fig. 7. Linear interpolation of average values of instantenous fuel consumption recorded on an engine test bench and calculated on the basis of parameters measured by the PEMS.

Table IV. Comparison of specific fuel consumption and overall efficiency of tested engine

Engine speed (rpm)	Torque (Nm)	BSFC (g/kWh)	Efficiency (%)
900	0	–	–
1800	0	–	–
	20	295.3	28.6
	40	285.6	28.7
	60	266.4	30.7
	80	258.5	31.7
	100	250.8	32.6
2200	0	–	–
	20	368.4	22.4
	40	275.5	29.8
	60	238.5	34.5
	80	228.3	35.9
2600	0	–	–
	20	384.4	21.3
	40	283.6	20.1
	60	243.8	33.7
	80	237.3	34.5

was recorded for S = 2200 rpm and loads of 60 Nm and 80 Nm, with efficiency of 34.5% and 35.9%, respectively. For S = 1800 rpm and T = 100 Nm, the overall efficiency was 32.6%, whereas for S = 2600 rpm and T = 69 Nm, it amounted to 33.7%. For idling (the lowest possible speed of the crankshaft without load) and neutral (increased speed of the crankshaft without load), the BSFC and efficiency were not calculated, because the engine does not generate any power output for transmission to the receiver. It only generates power as needed to overcome the resistance of its operation. Due to the existence of these points in the real road driving conditions, it was decided to also include these points in the analysis. In these cases, only the value of the power generated by ATEG is presented, without determining its effect on overall engine efficiency.

The ATEG power was determined based on the measured voltage and current generated by the thermoelectric modules at each measurement point. The tests began with the engine stabilized thermally and with generator wall temperature not exceeding 50°C. The duration of the measurement at each point was 60 s to 90 s. Before recording the parameters after setting the operating point of the engine, the system was given time until temperatures on the walls of the ATEG stabilized. After this period, recording of working parameters was performed. This scheme was adopted in each load characteristic. When changing the range of crankshaft speed, the ATEG conditioning time was significantly prolonged to lower the temperature of its walls to fixed values. This measure was used to reduce the impact of the thermal capacity of the aluminum on the heat flux from the exhaust gases conducted to the thermoelectric modules. Due to the number of measurements and the measured parameters, only exemplary temperature distributions for the exhaust system and on the walls of the heat exchanger (hot side of the thermoelectric modules) are presented herein. Measurements were carried out using water from the sanitary system as coolant with temperature of 10°C to 12°C at volumetric flow rate of ~0.045 m^3/h.

For neutral gear at S = 1800 rpm, the exhaust gas temperature between the turbocharger and the catalytic converter averaged 421.5°C throughout the duration of the measurement (Fig. 8). The ATEG was placed at a distance of ~1.5 m from the end of the catalytic reactor's confusor. The inlet temperature to the generator averaged 91.4°C. The temperature drop in the generator was 30.3°C. At maximum load (100 Nm) for the same rotational speed of the engine crankshaft, this drop was 140.8°C, and the average temperature on the input was t_4 = 491.5°C.

For the above measuring point, the highest temperature was recorded on the bottom wall of the heat exchanger (a substantial part of the ATEG), being equal to t_{51} = 45.5°C (Fig. 9). The minimum temperature value recorded occurred at the point t_{11}. The temperature difference between these two points was 7°C. This temperature difference is not very significant, meaning that the thermoelectric modules generated similar voltage and current values. Considering the temperature distribution on the walls of the ATEG along each row of modules, it was found that the greatest temperature drop occurred on the left side wall of the generator: $\Delta t_3 = t_{31} - t_{32}$ = 6.4°C. On other walls, the recorded temperature differences varied within the range of 0.3°C to 4°C. In the case of maximum load (with S = 1800 rpm), the highest temperature also occurred at the point t_{51} and was equal to 175°C.

To determine the effect of the ATEG on the total efficiency of the tested engine based on the data at these measuring points, it was first necessary to determine the power generated by the thermoelectric modules P_{eATEG} using the values of voltage and

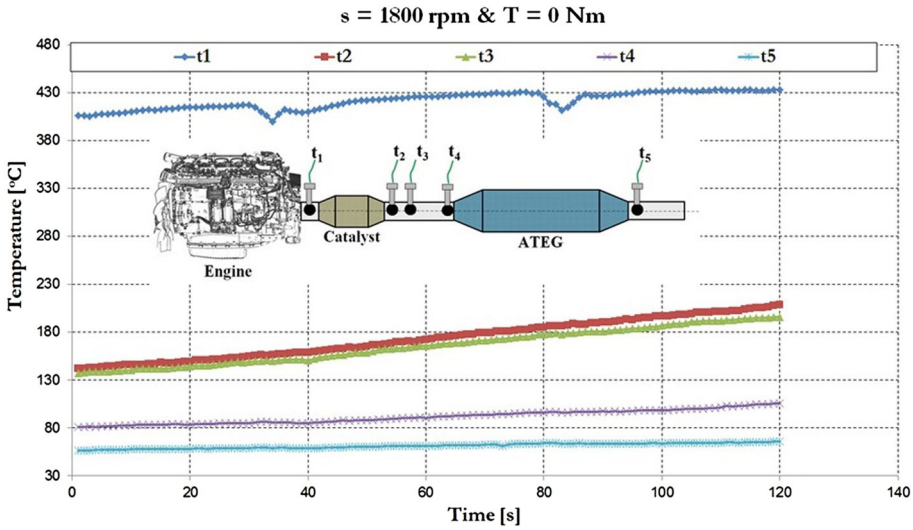

Fig. 8. Temperature distribution in exhaust system of tested engine with ATEG for neutral gear at S = 1800 rpm.

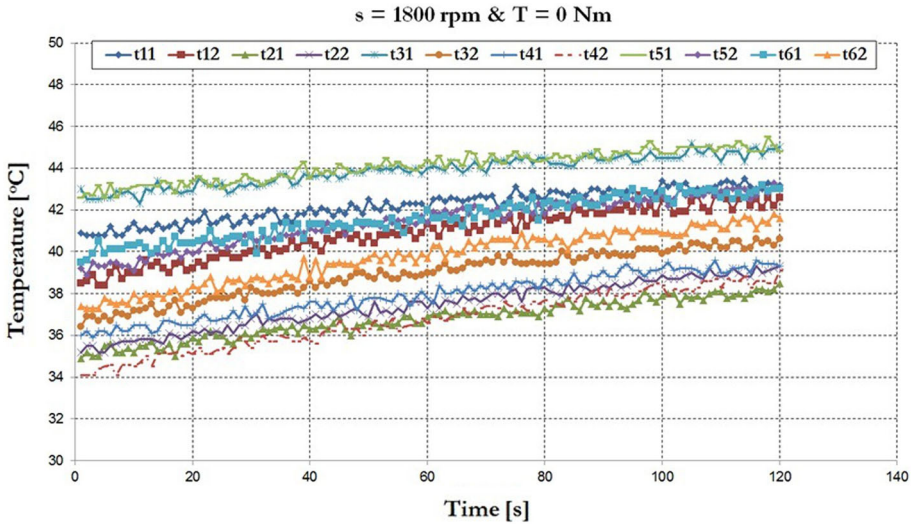

Fig. 9. Temperature distribution on a substantial part of the ATEG heat exchanger–hot side of the thermoelectric modules for neutral gear at S = 1800 rpm.

current obtained using the developed measurement system. At all the load characteristics, a trend of increased ATEG power generation with increasing engine torque (Fig. 10) could be observed. This is logical because, at higher loads, the engine produces more exhaust gases at higher temperature. The highest values of P_{eATEG} were as follows:

(a) 90.1 W at 1800 rpm
(b) 98.8 W at 2200 rpm
(c) 189.3 W at 2600 rpm

For engine idling (S = 900 rpm and T = 0), P_{eATEG} did not exceed 1 W. The obtained test results did not reach the ATEG nominal power, which is equal to 225.6 W. The system generated at most 84% of its maximum nominal power.

The overall engine efficiency, including the energy generated by the ATEG, was determined using Eq. 2. Then, the obtained values were compared with the determined total engine efficiency (Table IV). According to this assessment, the greatest efficiency improvement was obtained for S = 2600 rpm (Fig. 11). The energy generated by the ATEG over the tested range of engine operation does not constitute a significant share of the total energy. This is mainly a result of the failure to achieve the nominal power of the generator. The analysis above does not take into account the power loss occurring in the ATEG associated with resistance to the flow of exhaust gases.

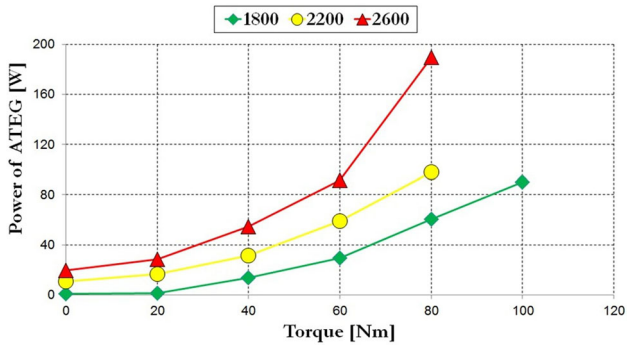

Fig. 10. Calculated power generated by the thermoelectric generator modules (ATEG) during tests.

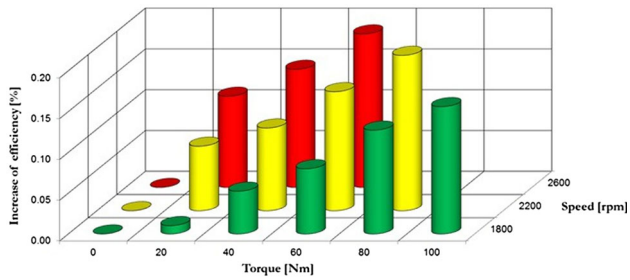

Fig. 11. Increase in overall efficiency of test engine through application of ATEG in exhaust system.

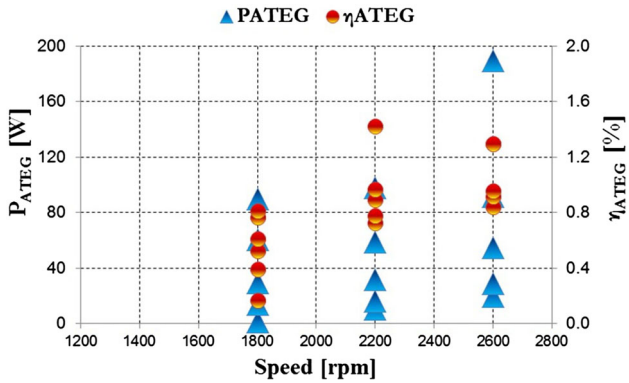

Fig. 12. Power and efficiency of ATEG depending on engine speed.

To determine the efficiency of the ATEG in terms of conversion of exhaust gas thermal energy into electrical energy, one needs to determine the amount of thermal energy from the relation

$$Q_{\mathrm{EXHAUST}} = \dot{m}_{\mathrm{EX}} \cdot c_{\mathrm{pEX}} \cdot \Delta T_{\mathrm{EX}}, \tag{3}$$

where Q_{EXHAUST} is the exhaust gas energy losses (enthalpy) (kW), $\dot{m}_{\mathrm{EX}}$ is the exhaust gas mass flow (kg/s), c_{pEX} is the exhaust gas specific heat at constant pressure [kJ/(kg K)], and ΔT_{EX} is the exhaust gas temperature (K). The ATEG efficiency η_{TEG} was determined from the relation

$$\eta_{\mathrm{TEG}} = \frac{P_{\mathrm{ATEG}}}{Q_{\mathrm{EXHAUST}}}, \tag{4}$$

where η_{TEG} is the efficiency of the ATEG (%), P_{TEG} is the ATEG power (W), and Q_{EXHAUST} is the exhaust gas energy losses (enthalpy) (W).

In determining the efficiency η_{ATEG}, the power losses resulting from the exhaust gas flow resistance inside the heat exchanger were not taken into account. For the load characteristics at S = 1800 rpm, the maximum efficiency η_{ATEG} did not exceed 0.8% (Fig. 12). For the other load characteristics, this efficiency was between 0.5% and 1.3%.

CONCLUSIONS

We present a study of the impact of a prototype ATEG on the overall efficiency of a modern SI engine designed in accordance with downsizing principles. The walls of the ATEG exhibited an almost uniform temperature distribution, both along and between the walls. Temperature differences amounted to a maximum of 7°C for neutral gear, being larger for higher loads. The measuring points did not reach the maximum power output of the ATEG. Only for S = 2600 rpm and T = 80 Nm was more than 80% of the nominal power output achieved. Energy losses arising as a result of the flow resistance of exhaust gases in the heat exchanger of the generator were not accounted for in this research. The authors plan to conduct further research including:

(a) Performance measurements of heat energy recovery using the designed prototype ATEG system at operating points reflecting rural and highway driving conditions,
(b) Determination of the energy losses due to the flow resistance of exhaust gases through the heat exchanger,
(c) Adjustment of the design and construction of the ATEG to further increase the efficiency of heat recovery from exhaust gases,
(d) Integration of the ATEG cooling system with that of the vehicle.

ACKNOWLEDGEMENTS

The research was funded by the National Centre for Research and Development (Narodowe Centrum Badań i Rozwoju) research project within the Applied Research Programme (Contract No. PBS1/A6/7/2012).

OPEN ACCESS

REFERENCES

1. F. Aren, L. Mezzan, A. Doyon, H. Suzuki, K. Lee, and T. Becker, *The Automotive CO_2 Emissions Challenge. 2020 Regulatory Scenario for Passenger Cars* (Arthur D. Little, Rome, 2014). http://www.adlittle.com/downloads/tx_adlreports/ADL_AMG_2014_Automotive_CO2_Emissions_Challenge.pdf.
2. European Commission, *Communication from the Commission to the European Parliament, the Council, the European Economic and Social Committee and the Committee of the Regions. An Integrated Industrial Policy for the Globalisation Era Putting Competitiveness and Sustainability at Centre Stage*. (European Commission, Brussels, 2010) http://eur-lex.europa.eu/LexUriServ/LexUriServ.do?uri=CCO:2010:0614:FIN:EN:PDF.
3. M. Brzeżański and K. Śliwiński, *Combust. Engines*. 119 (2004).
4. M. Bajerlein and L. Rymaniak, *Appl. Mech. Mater.* 518, 96–101 (2014).
5. P. Bombard, C.M. Invernizzi, and C. Pietra, *J. Electron. Mater.* (2010). doi:10.1016/j.applthermaleng.2009.08.006.
6. J. Dong, Y.J. Wang, R. Zhang, and B. Wang, *J. Electron. Mater.* (2014). doi:10.1007/978-3-662-45043-7_15.
7. N. Espinosa, M. Lazard, L. Aixala, and H. Scherrer, *J. Electron. Mater.* (2010). doi:10.1007/s11664-010-1305-2.
8. J. Merkisz, P. Fuc, P. Lijewski, A. Ziolkowski, and K.T. Wojciechowski, *J. Electron. Mater.* (2015). doi:10.1007/s11664-014-3522-6.
9. K. Shiho, P. Soonseo, K. SunKook, and R. Seok-Ho, *J. Electron. Mater.* (2011). doi:10.1007/s11664-011-1580-6.
10. D. Tatarinov, M. Koppers, G. Bastian, and D. Schramm, *J. Electron. Mater.* (2013). doi:10.1007/s11664-013-2642-8.
11. SEMTECH® ECOSTAR (Gaseous). Getting Started. Quick Reference Manual. Document: 9510-159 (Sensors Inc., USA, 2014).
12. J. Merkisz, P. Fuc, P. Lijewski, and A. Ziolkowski, *Appl. Mech. Mater.* 390, 343–349 (2013).
13. Thermoelectric module TMG-241-1.4-1.2 SCTB NORD A Ferrotec Group Company.
14. Fuc, J. Merkisz, P. Lijewski, A. Merkisz-Guranowska, and A. Ziolkowski, in *Energy Production and Management in the 21st Century: The Quest for Sustainable Energy (Volume 1)*, ed. C.A. Brebbia, E.R. Magaril, and M.Y. Khodorovsky (WIT Transactions on Ecology and the Environment, New Forest, 2014), pp. 369–378.